

Multifunctional and Low-Density Inorganic Nanocomposites

DANIEL M. DABBS^{1,2} and ILHAN A. AKSAY^{1,3}

1.—Department of Chemical and Biological Engineering, Princeton University, Princeton, NJ 08544, USA. 2.—e-mail: ddabbs@princeton.edu. 3.—e-mail: iaksay@princeton.edu

We summarize our recent studies on the use of low-density nanoporous silica structures prepared through templating of a self-assembling disordered liquid-crystalline L_3 phase, as a matrix for use in numerous applications, including sensing, optical data storage, drug release, and structural. The silica matrix exhibits low density (0.5 g cm^{-3} to 0.8 g cm^{-3} for monoliths, 0.6 g cm^{-3} to 0.99 g cm^{-3} for fibers) coupled with high surface areas (up to $1400 \text{ m}^2 \text{ g}^{-1}$) and void volumes (65% or higher). High-surface-area coatings are used to increase the sensitivity of mass-detecting quartz crystal microbalances to over 4000 times that of uncoated crystals. Monoliths, films, and fibers are produced using the templated silica gel. Once dried and converted to silica, the nanostructured material exhibits high fracture strength (up to 35 MPa in fibers) and Young's modulus (30 GPa to 40 GPa in fibers). These values are, respectively, two orders of magnitude and twice those of nanostructured silicas having comparable densities.

NATURAL AND SYNTHETIC MULTIFUNCTIONAL LIGHTWEIGHT MATERIALS

Natural cellular materials such as cancellous bone¹ (Fig. 1a)² and wood (Fig. 1b) provide excellent models for strong and tough materials that are lightweight (densities below 1 g cm^{-3}) and durable while supporting a channel network for efficient transport of fluids throughout. The open channel network in natural materials is vital for multifunctionality and self-repairing mechanisms.³ The hierarchical control of composite synthesis and architecture over multiple scales of dimension (from Angstroms to centimeters) and at ambient temperatures is one of the most remarkable features of biological structures.^{4,5} A hierarchical biocomposite is more than just a material out of which larger objects can be built: it is a complete structural system in itself.⁴ Bone is of special interest as it is an inorganic–organic nanocomposite, a rich source for the bio-inspired design of structures and functional properties in synthetic materials. As a purely organic material, wood remains the most widely used structural material, exhibiting physical properties difficult to match with synthetic materials.^{6,7} Like bone, the cell walls of wood are hierarchically structured, a fiber-reinforced composite consisting of

cellulosic fibers embedded in a matrix of semiamorphous hemicellulose and amorphous lignin.^{8–10}

Our interest in hierarchically structured nano- to microporous materials is due to their potential role as building blocks in adaptive materials.* We view the use of cellular or porous structures as an essential structural feature for multifunctionality in order to transport mass through a fluid phase rapidly, rather than relying on the slow solid-state transport processes of fully dense solid structures. We contend that such nanoporous structures can be built using self-assembling liquid-crystalline templates as scaffolds for deposition and subsequent conversion of metal alkoxides to metal oxide nanostructures, especially advantageous for fabricating highly porous materials (Fig. 2).^{11–16} Templation has been used to fabricate nanostructured materials

*The goal of our Army Research Office (ARO)-sponsored Multidisciplinary University Research Initiative (MURI) program on Adaptive Structural Materials (grant #W911NF-09-1-0476) is to develop responsive materials for sensing stress/strain variations in load-carrying components of structural materials and couple sensory output to adaptive functionalities. Cellular or porous structures similar to bone are an essential element of the structures under development, needed to facilitate rapid transport of mass to stressed regions using a fluid phase, thereby avoiding slow solid-state mass transport.

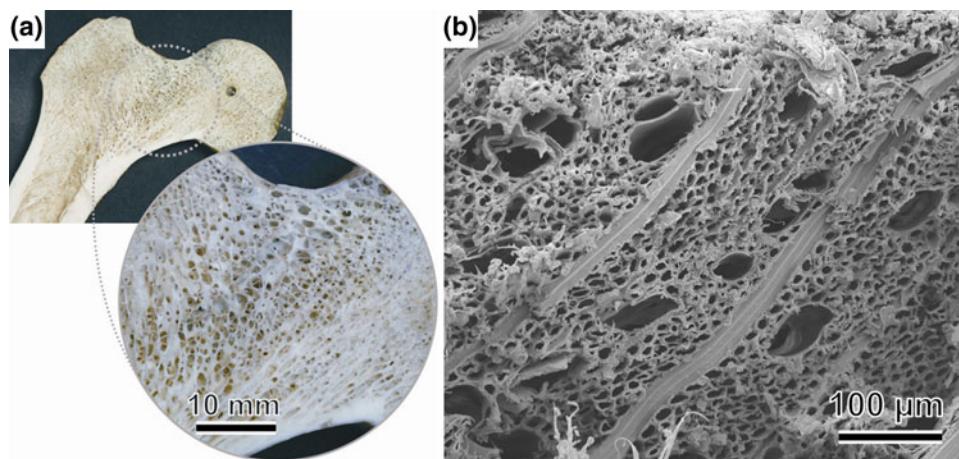


Fig. 1. (a) Hierarchically porous structure of bone. In this microscopic image, the parts of the bone that are more stressed are more dense, while the central zone which carries less load is highly porous and open for transport of fluids. (b) Wood is composed of a highly oriented series of channels, seen here in the axial or cross-grain plane, giving wood a strong and tough structure that also provides for rapid exchange of fluids within the tree [maple in this example; sample freeze-fractured for scanning electron microscope (SEM) analysis].

with large, connected void volumes¹⁷ composed of channels of uniform size.^{18–21} While we have looked into the synthesis of various phases (e.g., lamellar, hexagonal, cubic),^{22,23} here we specifically focus on the applications of nanostructured silica powder and monoliths using the disordered and isotropic L_3 liquid-crystalline phase²⁴ as the template (Fig. 2c), since this phase provides a bicontinuous void volume with no domain boundaries.²⁵ The absence of domain boundaries is especially useful in optical applications.²⁶ Further, our approach eliminates many of the disadvantages of other surfactant-formed nanostructures, such as limitations on the size of the template that can be formed and the need to remove the surfactant to open the primary channels following templation, as the silica walls encapsulate and isolate the organic template. Whether as monoliths, powders, coatings, or fibers, our L_3 -templated silica has surface areas comparable to those of silica aerogels, up to $1400 \text{ m}^2 \text{ g}^{-1}$ as determined by Brunauer–Emmett–Teller (BET) sorption measurements.^{18–21} Monoliths (such as the one shown in Fig. 3a) of L_3 -templated silica have tunable densities ranging from 0.5 g cm^{-3} to 0.8 g cm^{-3} .^{18–21} We have also shown that L_3 -templated silica monoliths are mechanically robust and can be infiltrated with liquids after drying, a necessary step for introducing functionalities needed for sensing^{20,21} and optical applications.²⁶

THE L_3 PHASE AND THE SYNTHESIS OF L_3 -TEMPLATED SILICA MONOLITHS

With the L_3 phase, very large channels can be produced as the pore size is determined by the relative concentration of the constituents and not the length of the surfactant.^{18,19} Unlike silica xerogels (Fig. 2a) and aerogels, there is little variation in the diameter of the channels. The ordered structure of the hexagonal phase (Fig. 2b) results in the

formation of domains that restrict access to the channels and so reduce the useful exposed surfaces. In contrast, solutions of the L_3 crystalline phase are optically isotropic and clear, retaining optical clarity in the L_3 -templated silicas, whether or not the organic components are removed from the solid.^{18,19} The channel structure is tunable, in that the average channel diameter can be varied from 1 nm to 100 nm simply by changing the ratio of the solvent (water) to the nonpolar constituents.^{18,19}

The procedure for making L_3 silica gels has been described in several articles and will not be repeated here.^{18–21,26} Hexanol, tetramethoxysilane (TMOS), cetylpyridinium chloride monohydrate (CpCl·H₂O), absolute ethanol and methanol, and stock solutions of 0.2 M hydrochloric acid prepared from reagent-grade HCl (aq) diluted with deionized (DI) water are used in the synthesis. The L_3 liquid-crystalline phase spontaneously forms when the appropriate ratio of hexanol and CpCl (~ 1.15 hexanol/CpCl·H₂O by weight) is added to a 0.2 M solution of chloride in water. The source of the chloride ion is not important, and this allows the pH of the liquid-crystalline solution to be tuned to better control the hydrolysis and condensation of the TMOS when it is added to the liquid-crystalline solution.²⁰ The gels become rigid within 48 h to 96 h of adding TMOS at room temperature, the amount of time needed depending on the temperature, the amount of TMOS added, and the pH of the L_3 solution.²⁶ Following supercritical extraction (SCE), the L_3 -templated silica has high surface area ($1000 \text{ m}^2 \text{ g}^{-1}$ to $1400 \text{ m}^2 \text{ g}^{-1}$) and void volume ($\sim 65\%$).²⁶

MULTIFUNCTIONALITY OF L_3 -TEMPLATED SILICA

The open isotropic structure of the L_3 -templated silica (Fig. 2c) resembles the structure of cancellous bone (Fig. 1a), with rigid struts defining a

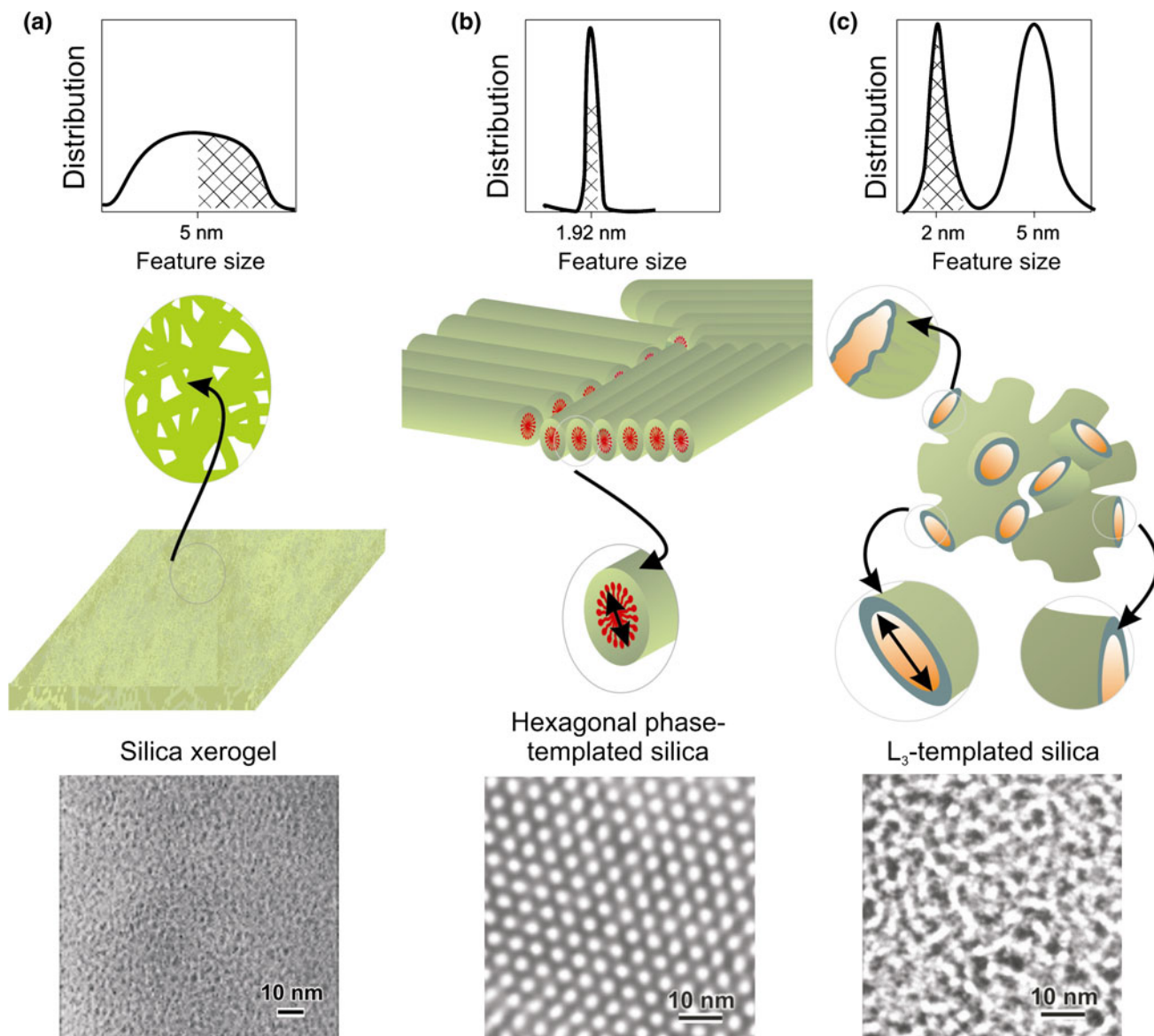


Fig. 2. Characteristic size distributions (top), schematics of structures (middle), and transmission electron microscope (TEM) images (bottom) of (a) a silica xerogel, (b) hexagonal phase-templated silica, and (c) L_3 -templated disordered silica. The shaded regions of the size distributions represent *inaccessible* regions within the nanostructure. The most prominent feature size is the diameter of the channels (1.92 nm for hexagonal phase-templated silica and 5 nm for the L_3 -templated silica). For the L_3 -templated silica, the surfactant bilayer has a dimension of 2 nm (adapted from Bhansali et al.)²¹.

continuous void volume. Like bone, this structure implies mechanical robustness coupled with high flow rates for fluid phases that can penetrate into a significant fraction of the structure. The lack of domains, due to its disordered structure, improves fluid flow through a multitude of paths that are continuous throughout.²⁷ The combination of rapid fluid penetration and flow with mechanical robustness allows other materials to be readily introduced into the structure. This may be used to modify the silica walls to improve mechanical properties or to add chemical functionalities to the nanoporous structure to serve as catalytic and/or sensor sites.

Silica may also simply serve as a filter that operates within the so-called mesoscale (1 nm to 100 nm).

In the following sections, we report on several recent projects in which L_3 -templated silica shows potential as the matrix for applications in optics, sensors, drug delivery, and as a lightweight multifunctional structural material. Our goal for L_3 -templated silica-based materials is to use the nanoporous frame as the basis for developing a load-bearing smart structure whose members can be modified to provide other functions, such as sensing or catalyst, while maintaining an open structure for material transport.

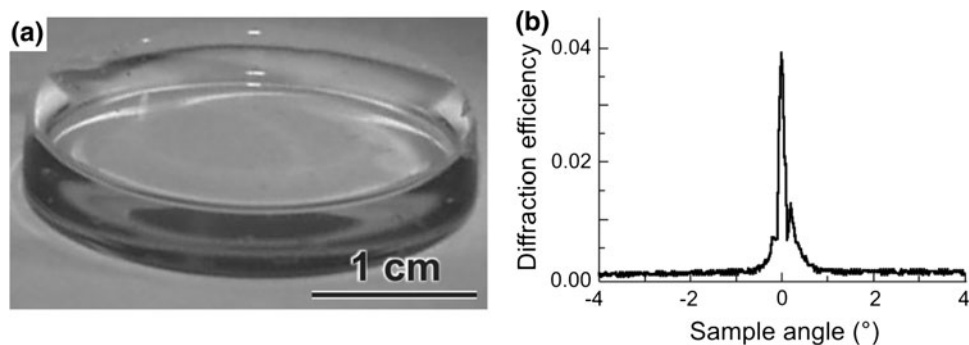


Fig. 3. (a) A representative disk of L_3 -templated silica after supercritical ethanol extraction.²⁶ The original gel was cast into the shape of a disk into a Petri dish, and the rim at the edge was caused by the wetting of the dish by the gel while still fluid. (b) A representative Bragg peak obtained from a photomonomer-filled L_3 -templated silica disk. The volume that produces the diffraction peak was produced by the crossed lasers polymerizing the monomer in a specific volume of the disk.

Optical Data Storage Using Photopolymers in a Nanoporous Matrix

Due to its optical transparency and the dimensional stability inherent in a nanoporous material with a well-connected frame, an obvious function for L_3 -templated silica is in optics. Towards this goal, we work with large disks (3 cm diameter, 0.5 cm thick) of L_3 -templated silica made by SCE of the organic components from the cast silica using ethanol as the extracting solvent (Fig. 3a). The rigid, porous structure is useful as a potential three-dimensional optical storage device.²⁶ It is robust enough to withstand subsequent infiltration by liquids. This attribute is used to good effect by infiltrating these large disks first with an acrylate monomer, followed by *in situ* polymerization of the monomer without damaging the disks. Conversion to a polyacrylate within the channels creates an organic-inorganic composite with nanoscale features, itself of interest for composite structures, but also provides a proof of concept for the fabrication of holographic data storage media.

Photopolymer composites consist of a photoactive component, such as a monomer, that is held within the void volumes of a matrix.²⁸ Two lasers held at different angles to the matrix are then crossed at selected sites within the matrix to produce a two-photon process that selectively cures or polymerizes the active agent within a small volume.²⁹ Modulating one laser with the second allows the patterning of an optical grating with both spatial and angular dependence. An original pattern is recovered by reading the grating using a single laser held at the same angle as the modulating laser that was used to write the grating. Varying the angle of the two beams during the writing process allows several such gratings to be written within the same spatial volume, the information (that is, the gratings) separated from each other corresponding to the Bragg effect.³⁰ To maintain the separation between the gratings the matrix is ideally rigid, maintaining the spatial and angular locations created for each grating. An SCE-treated L_3 -templated silica disk

infiltrated with a photomonomer and photoinitiator and then exposed to crossed lasers produces a grating that is subsequently rendered visible by means of the diffraction of a single laser at the correct angle to the sample (Fig. 3b). The matrix remains visibly transparent, and the sample's dimensional stability permits accurate reading of the test grating over a wide range of temperatures.²⁶ Although this has not been reduced to data storage applications at this time, the ability to write a grating into the nanostructured silica demonstrates that both the monomer and initiator completely and uniformly fill the channels of the matrix, permitting single gratings to be written at different volumes within the photocomposite.

Enhanced Sensitivity Through Nanoporous Coatings

Increasing the amount of a substance that can be imbibed by a structure can be accomplished by simply increasing the void volume and the exposed surface area of the composite material. The increased surface area and the high transport volumes offered by such structures can then be used to increase the amount of substances adsorbed onto an active surface from gas or liquid phase. To demonstrate the point, we increase the sensitivity of the commonly used single-crystal quartz resonators, the quartz crystal microbalance (QCM), to the presence of a gaseous species (e.g., water vapor or ethanol in the gas phase) by applying an L_3 -templated silica coating to the measuring side of the QCM (Fig. 4), determined by the mass accumulation isotherms across a range of the targeted molecule's vapor partial pressures.^{21,31} Comparing QCMs coated with 1- μm -thick coatings of either silica xerogel, hexagonal-phase templated silica, or L_3 -templated silica (Fig. 2), we find that (i) QCMs coated with hexagonal phase-templated silica are 100 times more sensitive to the presence of water vapor compared with an uncoated QCM, whereas (ii) L_3 -phase templated silica coatings on QCMs result in a composite up to 4000 times more sensitive to water

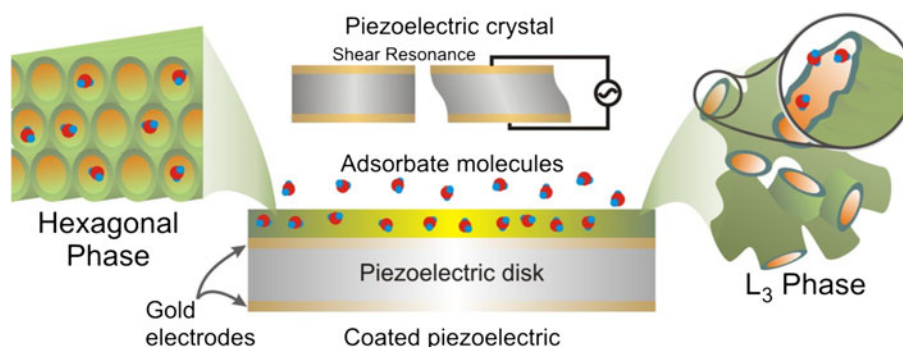


Fig. 4. Schematic of a sensing system using either hexagonal-phase- or L_3 -templated coatings on piezoelectric crystals to increase the sensitivity of the resonator by increasing the volume for mass accumulation.^{20,31} The shear resonance of the piezoelectric crystal, such as a gold-coated QCM as discussed in the text, is affected by the mass of the material adsorbed on the sampling (coated) surface. Despite the mass of the coating itself, the increase in surface area permits a much higher amount of the targeted molecule to be adsorbed, and the sensitivity of the sensor is enhanced. As shown in the schematic, the targeted molecule here is water, but functionalizing the nanostructured silica using specialized receptor molecules, such as the calixarenes described in the text, would extend this system to other substances.

vapor than the uncoated QCM. Three characteristics of the coatings are determined to affect the overall sensitivity of the coated resonator: (i) the specific surface area per unit mass of the coating, (ii) the accessibility of the surfaces to the targeted molecules, and (iii) the distribution in the characteristic radii of curvature of internal surfaces, as measured by capillary condensation. When comparing the structures of the hexagonal and L_3 -templated silicas (Fig. 2), it is obvious that the isotropic structure of the L_3 provides ready access to the void volume at any orientation. Increasing specific surface area enhances mass accumulation via the formation of monolayers at low partial pressures ($P/P_0 < 0.2$),³² but channel uniformity and access are most significant in determining mass accumulation at greater partial pressures ($P/P_0 > 0.2$), a region of multilayer formation (the BET model)³³ and where capillary condensation can occur.³⁴ Using the point at which capillary condensation occurs in hexagonal- or L_3 -phase-templated silica coatings, the L_3 -templated silica has a much higher radius of curvature in its channels, 2.5 nm, than does the hexagonal-phase-templated silica, 0.96 nm. Use of both specific surface area and uniformity of the nanostructure to enhance resonator sensitivity is only possible provided the nanostructures within the films are accessible to the target molecules and the increased accessibility of the L_3 -templated silica is apparent in the larger amount of water accumulated with respect to hexagonal-phase-templated silica (for example, at partial pressures of 0.7, the L_3 coating accumulates 0.473 g of water per gram of coating; the hexagonal phase only 0.146 g of water per gram of coating).²¹

In addition to using L_3 -templated silica coatings to provide a higher surface area for adsorption, the walls of the nanostructured silica provide an appropriate substrate onto which responsive molecules (receptors) can be attached; For example, the L_3 -templated silica has been shown to provide a suitable substrate for grafting of calixarenes.³⁵

Calixarenes are a cup-shaped class of molecules that can be tuned to selectively adsorb targeted organics, known to readily bind to silica surfaces.³⁶ When grafted onto silica, the molecules are rigidly immobilized in their cone conformations at near-monolayer site densities, in a direction orthogonal to the silica surface.³⁶ Silica-based materials with calixarenes grafted onto the accessible surfaces exhibit hierarchical adsorption mechanics: silica surfaces not covered with calixarenes remain available for adsorption, with the calixarenes acting as receptors for specific target molecules. The two types of adsorbing sites are known to function independently,³⁷ but calixarene-coated silica surfaces also demonstrate a synergistic effect at the interface between the calixarene and silica. For example, the total amount of toluene adsorbed from the vapor state is greater than what is expected based on the number of calixarene sites on a silica surface plus the amount of uncovered silica exposed to toluene vapor. The calixarene-coated silicas adsorb 57% more toluene from the vapor phase than the untreated silica.³⁵

Combining the concepts of nanoporous structures with that of targeted adsorption through surface functionalization suggests linked arrays of microscale, tunable sensors. In a single-analyte sensor, a receptor molecule interacts with the targeted analyte in a detectable manner. A “multicomponent” analyzer built using sensors of this type would require multiple selective sensors, which would not be small or portable. An alternative approach is the fabrication of arrays of less specific sensor “pixels” that respond to a wider variety of functional groups, molecular structures, or elements, providing an electronic nose (detection in air) or tongue (detection in liquid). The heart of this system would be patterned arrays of microscale piezoelectrics produced by sol-gel micropatterning methods,^{38–41} such as lead zirconate titanate [$\text{Pb}(\text{Zr}_{0.52}\text{Ti}_{0.48})\text{O}_3$ (PZT)] as miniaturized piezoelectric crystal balances (analogous to the QCMs discussed above). These

microelectrodes can be coated with L_3 -templated silica layers, and groups of the coated piezoelectrics functionalized with appropriate receptors to enhance chemical selectivity and sensitivity. Such arrays combine four areas under current investigation: (i) micromolding of PZT microarrays using PZT-precursor liquid solutions,⁴¹ (ii) nanoporous silica coatings (described above), (iii) directed assembly of nanostructured layers into arrays, and (iv) structuring of self-assembled monolayers on nanoporous silica. For miniaturization, sol-gel processing of PZT piezoelectrics³⁸⁻⁴¹ remains the most promising for a truly all-electronic system. In contrast, piezoelectric structures machined from single crystals such as quartz crystal microbalances are not easily fabricated at the micrometer scale.

Controlled Drug Delivery Using Thermoresponsive Nanocomposites

The examples described in the previous sections depend on getting fluids into the nanostructure but have not dealt with the issue of getting materials out in a controlled manner, a process vital for catalytic, drug release, or sensing applications. Controlled release is an application that first relies on filling the channels of the L_3 -templated silica with an active agent to form a composite as previously described. Then, the open structure of the silica can be used to maintain a steady release of a specific compound while the overall structure of the composite remains unchanged. A significant example is smart drug delivery, which depends on controlled release of a drug over time, where the amount released to the body remains fairly constant over the lifetime of the drug-delivery system, avoiding sudden changes in the amount of drug delivered. The isotropic random structure of L_3 -templated silica provides a suitable matrix for drug delivery as silica is reasonably inert and the channel structure open to filling with a liquid or melt.

The fabrication of a responsive or adaptive material has been demonstrated by filling the channels of L_3 -templated silica with the thermoresponsive polymer poly(*N*-isopropylacryl amide) (PNIPAm), creating a composite material of filled L_3 -templated silica (L_3 -PNIPAm). Adding the PNIPAm results in a dramatic decrease in the available surface area from that of the L_3 -templated silica alone:⁴² for L_3 -templated silica containing 95 wt.% water, the measured BET surface area falls from $522 \text{ m}^2 \text{ g}^{-1}$ to $35 \text{ m}^2 \text{ g}^{-1}$ for the L_3 -PNIPAm gels with equivalent water content, indicating that the channels of the L_3 -templated silica were modified by coating with PNIPAm polymer. In addition, the estimated channel diameters of the L_3 -templated silica fall from 10 nm to ~ 6 nm following infiltration and polymerization of the PNIPAm gel.

The PNIPAm gel fills the channel network of the L_3 -templated silica skeleton, the gel then providing a medium for storing the antipyretic and analgesic

drug indomethacin (IMC) within the L_3 -PNIPAm.⁴² Stepwise temperature changes from ambient to 40°C and back to ambient cause the PNIPAm gel within the silica matrix to contract and expand. Raising the temperature contracts the gel, causing a squeezing mechanism that releases the IMC into the channels; the IMC is subsequently transported from the L_3 -PNIPAm composite into the environment. In the test, the IMC-containing L_3 -PNIPAm composite is held at 25°C ("off") for 24 h, then heated to and held at 40°C for 24 h ("on"). This off-and-on cycle is repeated over 10 days, and the cumulative amount of IMC released recorded at intervals of several hours. When "off," the cumulative amount of IMC was much less than 0.1 mg per g of composite after 24 h. When "on," the cumulative amount of IMC released over 24 h rose to 0.3 to 0.5 mg per g of composite. The rate of IMC release and the cumulative amount released over 24 h remain remarkably consistent over the 10 days, despite the decreasing IMC content of the PNIPAm, perhaps explained by reopening of L_3 channels through the loss of volume in the incorporated PNIPAm gel as the amount of drug in the gel decreases. Thus a controllable drug-delivery system can be designed using a porous ceramic matrix containing a responsive or degradable polymer. Using a responsive material to fill the channels, such as the thermoresponsive PNIPAm, application of the appropriate stimulus releases the active agent, in this example the IMC, and the L_3 -PNIPAm composite can then be classified as an adaptive material, one that reacts in a predetermined manner to changes in its environment.

High-Strength Fibers and Adaptive Textiles

Other than noting the ability to imbibe liquids or vapors into the L_3 -templated silica framework, the applications described in previous sections do not focus on the mechanical properties of the L_3 -templated silica. An advantage frequently cited by us^{15,18,19,26} and others²⁷ for disordered structures including the L_3 -templated silica over that of other porous silicas (such as aerogels and hexagonally templated silica) is the assumed improvement in mechanical properties due to (i) the uniformity of the silica walls, (ii) the improved connectivity within the walls, and (iii) the continuity of the silica framework.¹⁸⁻²⁰ Beyond the application in large monolithic composites, as done for the optically active polymer/silica composites described above, monoliths⁴³ and fibers⁴⁴ of nanostructured silica also provide a matrix for incorporating active agents that could be used for optical transmission, sensing, or energy generation. Such smart fibers have recently become an active area of research, especially in the use of smart fabrics as a power source for personal electronic devices⁴⁵ and sensing systems.⁴⁶ Small-diameter fibers have the advantage that they can be woven or bundled into larger structures, providing flexibility to a material while reducing bulk.

To extend the utility of the L_3 -templated silica to adaptive textiles, we use L_3 -silica precursor gels to draw low-density fibers with high surface areas and tensile strengths up to 350 MPa, significantly higher than reported tensile strengths for aerogels and xerogels.^{43,44} As silicified liquid-crystal gels, there is a period during which fibers can be drawn from the thickening gel simply by pressing a glass rod into the gel and then pulling out a continuous fiber, up to 8 cm long to date (Fig. 5).⁴⁴ During drying, these fibers shrink in diameter, reaching final diameters of $\sim 100 \mu\text{m}$ (Fig. 5). For the bulk fibers, BET surface areas range from $450 \text{ m}^2 \text{ g}^{-1}$ to $600 \text{ m}^2 \text{ g}^{-1}$ following low-temperature ($< 500^\circ\text{C}$) heat treatment that helps to open the channels and reduce the organic content. Fiber densities range from 0.6 g cm^{-3} to 0.99 g cm^{-3} , and the final density can be controlled by the amount of TMOS added to the liquid-crystalline solution and the amount of water in the original solution. The fracture strengths up to 350 MPa under tensile testing are more than two orders of magnitude higher than the fracture strength of well-connected porous silicas of comparable density.^{43,44,47} Similarly, the Young's moduli for these fibers are also up to two orders of magnitude greater than those of other porous silicas,^{16,43,47} reaching values as high as 40 GPa under tension.

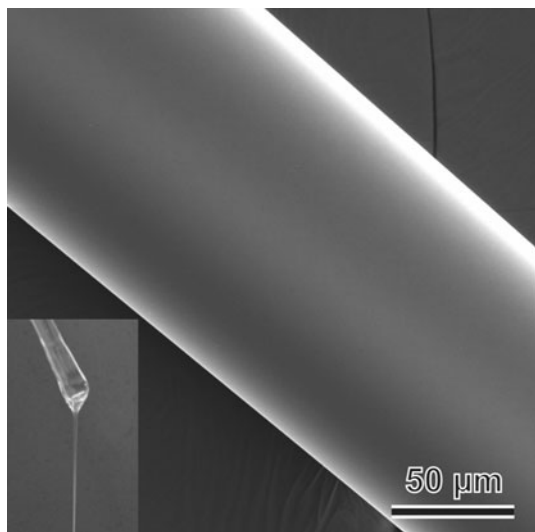


Fig. 5. Fiber drawn from L_3 -templated silica; typical densities were less than 1 g/cm^3 , and BET surface areas ranged from $450 \text{ m}^2/\text{g}$ to $600 \text{ m}^2/\text{g}$ following low-temperature ($< 500^\circ\text{C}$) heat treatment.⁴⁴ The lack of surface defects on the drawn fibers resulted in fracture strengths one to two orders of magnitude higher than those of nanostructured monoliths of comparable density. Young's moduli for the heat-treated fibers were two orders of magnitude higher than those for nanostructured monoliths of comparable density. Inset: A narrow window ($\sim 30 \text{ min}$) exists during which the gel is sufficiently viscous to be drawn into a fiber simply by contacting the gel with a glass rod and pulling. The time at which this window opens depends on the amount of TMOS added to the L_3 liquid-crystalline solution and the processing temperature, ranging from 36 h to 52 h at room temperature following TMOS addition

CONCLUSIONS

In the descriptions of the different uses of L_3 -templated silica, we have shown that the high void volume, surface area, and connectivity of the disordered channel network are well suited to the subsequent infiltration of such matrices by fluid phases, without compromising the structural integrity of the silica network. Whether as simple structural composites, optical components, sensors, or as a matrix for responsive materials, the strength and robustness of the L_3 -templated silica have been shown to provide an appropriate framework for developing lightweight multifunctional materials. The interconnectedness of the silica framework provides high mechanical strength, while the active, accessible surfaces of the channel walls provide sites for chemical reactions, permitting modification of the silica surfaces, implying that much more is to be done for use of these or similar materials in active filtration, catalysis, and sensing.

ACKNOWLEDGEMENTS

Aspects of the reported work were supported by grants from the Army Research Office Multidisciplinary University Research Institute (ARO/MURI; Grant No. W911NF-09-1-0476), and the Pacific Northwest National Laboratory (Grant No. DE-AC05-76RL01830).

REFERENCES

1. L.J. Gibson, *J. Biomech.* 18, 317 (1985).
2. E. Long (Senior Thesis, Civil Engineering and Operations Research, Princeton University, Princeton, 1997) (Advisor: J.-H. Prévost).
3. C.S. Chen and D.E. Ingber, *Osteoarthr. Articul. Cartil.* 1, 81 (1999).
4. *Hierarchical Structures in Biology as a Guide for New Materials Technology*, National Materials Advisory Board (Washington, D.C.: National Academy Press, 1994).
5. M. Sarikaya and I.A. Aksay, eds., *Biomimetics: Design and Processing of Materials* (Woodbury, NY: AIP Press, 1995).
6. *Wood Handbook: Wood as an Engineering Material*, General Technical Report FPL-GTR-190 (Madison, WI: Forest Products Laboratory, 2010).
7. P. Ball, *Nat. Mater.* 4, 515 (2005).
8. R.A. Parham and R.L. Gray, *The Chemistry of Solid Wood*, Adv. Chem. Ser. 207, ed. R. Rowell (Washington, DC: American Chemical Society, 1984), pp. 3–56.
9. D. Fengel and G. Wegener, *Wood: Chemistry, Ultrastructure, Reactions* (New York: Walter de Gruyter, 1984).
10. E. Sjöström, *Wood Chemistry: Fundamentals and Applications* (New York: Academic, 1981).
11. A. Corma, *Chem. Rev.* 97, 2373 (1997).
12. P.T. Tanev, M. Chibwe, and T.J. Pinnavaia, *Nature* 371, 321 (1994).
13. S.A. Bagshaw, E. Prouzet, and T.J. Pinnavaia, *Science* 269, 1242 (1995).
14. J.Y. Ying, C.P. Mehnert, and M.S. Wong, *Angew. Chem. Int. Ed.* 38, 56 (1999).
15. D.M. Dabbs and I.A. Aksay, *Annu. Rev. Phys. Chem.* 51, 601 (2000).
16. H. Fan, C. Hartshorn, T. Buchheit, D. Tallant, R. Assink, R. Simpson, D.J. Kissel, D.L. Lacks, S. Torquato, and C.J. Brinker, *Nat. Mater.* 6, 418 (2007).
17. C.T. Kresge, M.E. Leonowicz, W.J. Roth, J.C. Vartuli, and J.S. Beck, *Nature* 359, 710 (1992).

18. K.M. McGrath, D.M. Dabbs, N. Yao, I.A. Aksay, and S.M. Gruner, *Science* 277, 552 (1997).
19. K.M. McGrath, D.M. Dabbs, N. Yao, K.J. Edler, I.A. Aksay, and S.M. Gruner, *Langmuir* 16, 398 (2000).
20. S.H. Bhansali, A.-S. Malik, J.M. Jarvis, I. Akartuna, D.M. Dabbs, J.D. Carbeck, and I.A. Aksay, *Langmuir* 22, 4060 (2006).
21. S.H. Bhansali, J.M. Jarvis, I.A. Aksay, and J.D. Carbeck, *Langmuir* 22, 6676 (2006).
22. I.A. Aksay, M. Trau, S. Manne, I. Honma, N. Yao, L. Zhou, P. Fenter, P.M. Eisenberger, and S.M. Gruner, *Science* 273, 892 (1996).
23. M. Trau, N. Yao, E. Kim, Y. Xia, G.M. Whitesides, and I.A. Aksay, *Nature* 390, 674 (1997).
24. P. Pieruschka and S. Marcelja, *Langmuir* 10, 345 (1994).
25. D.M. Dabbs, N. Mulders, and I.A. Aksay, *J. Nanoparticle Res.* 8, 603 (2006).
26. A.S. Malik, D.M. Dabbs, H.E. Katz, and I.A. Aksay, *Langmuir* 22, 325 (2006).
27. D.R. Rolison, *Science* 299, 1698 (2003).
28. G.-D. Liu, Q.-S. He, S.-J. Luo, M.-X. Wu, G.-F. Jin, M.-Q. Shi, and F.-P. Wu, *Chin. Phys. Lett.* 20, 1733 (2003).
29. D. Psaltis and Fai Mok, *Sci. Am.* 273, 70 (1995).
30. H. Coufal, *Nature* 393, 628 (1998).
31. R.M. Kozarsky, *Enhancing the Sensitivity of Sensors Using Nanostructured Silica Coatings*, (Senior Thesis, Chemical Engineering, Princeton University, Princeton, 2007).
32. I. Langmuir, *J. Am. Chem. Soc.* 40, 1361 (1918).
33. S. Brunauer, P.H. Emmett, and E. Teller, *J. Am. Chem. Soc.* 60, 309 (1938).
34. K.S.W. Sing and R.T. Williams, *Adsorpt. Sci. Technol.* 22, 773 (2004).
35. Work done in collaboration with A. Katz, University of California, Berkeley (unpublished).
36. J.M. Notestein, A. Katz, and E. Iglesia, *Langmuir* 22, 4004 (2006).
37. J.M. Notestein and A. Katz, *Chem. Euro. J.* 12, 3954 (2006).
38. C.R. Martin and I.A. Aksay, *J. Mater. Res.* 20, 1995 (2005).
39. C.R. Martin and I.A. Aksay, *J. Electroceramics* 12, 53 (2004).
40. C.R. Martin and I.A. Aksay, *J. Phys. Chem. B* 107, 4261 (2003).
41. J.S. Vartuli, M. Ozenbas, C.M. Chun, M. Trau, and I.A. Aksay, *J. Mater. Res.* 18, 1259 (2003).
42. J.H. Chang, C.H. Shim, B.J. Kim, Y. Shin, G.J. Exarhos, and K.J. Kim, *Adv. Mater.* 17, 634 (2005).
43. H. Sai, *Mechanical Properties of L₃-Templated Nanostructured Silica* (Senior Thesis, Chemical Engineering, Princeton University: Princeton, 2007).
44. A.M. Pires, *Mechanical Properties of L₃-templated Silica Fibers* (Senior Thesis, Chemical Engineering, Princeton University, Princeton, 2010).
45. S. Egusa, Z. Wang, N. Chocat, Z.M. Ruff, A.M. Stolyarov, D. Shemuly, F. Sorin, P.T. Rakich, J.D. Joannopoulos, and Y. Fink, *Nat. Mater.* 9, 643 (2010).
46. A.F. Abouraddy, M. Bayindir, G. Benoit, S.D. Hart, K. Kuriki, N. Orf, O. Shapira, F. Sorin, B. Temelkuran, and Y. Fink, *Nat. Mater.* 6, 336 (2007).
47. T. Woignier, J. Reynes, A. Hafidi Alaoui, I. Beurroies, and J. Phalippou, *J. Non-Cryst. Solids* 241, 45 (1998).